Published in final edited form as:

Gene Ther. 2011 December ; 18(12): 1173–1178. doi:10.1038/gt.2011.118.

Imaging gene delivery in a mouse model of congenital neuronal ceroid lipofuscinosis

Lisa S. Pike[1,3], **Bakhos A. Tannous**[1,2,3], **Nikolaos C. Deliolanis**[a], **Gary Hsich**[1,b], **Danielle Morse**[1], **Ching-Hsuan Tung**[2,c], **Miguel Sena-Esteves**[1,d], and **Xandra O. Breakefield**[1,2]

[1] Department of Neurology, Massachusetts General Hospital and Neuroscience Program, Harvard Medical School, Boston, Massachusetts, USA

[2] Center for Molecular Imaging Research, Department of Radiology, Boston, Massachusetts, USA

Abstract

Adeno-associated virus (AAV) mediated gene replacement for lysosomal disorders have been spurred by the ability of some serotypes to efficiently transduce neurons in the brain and by the ability of lysosomal enzymes to cross-correct among cells. Here, we explored enzyme replacement therapy in a knock-out mouse model of congenital neuronal ceroid lipofuscinosis (NCL), the most severe of the NCLs in humans. The missing protease in this disorder, cathepsin D (CathD) has high levels in the central nervous system (CNS). This enzyme has the potential advantage for assessing experimental therapy in that it can be imaged using a near-infrared fluorescence (NIRF) probe activated by CathD. Injections of an AAV2/rh8 vector encoding mouse cathepsin D (mCathD) into both cerebral ventricles and peritoneum of newborn knock-out mice resulted in a significant increase in lifespan. Successful delivery of active CathD by the AAV2/rh8-mCathD vector was verified by NIRF imaging of mouse embryonic fibroblasts (MEFs) from knock-out mice in culture, as well as by *ex vivo* NIRF imaging of brain and liver after gene transfer. These studies support the potential effectiveness and imaging evaluation of enzyme replacement therapy to the brain and other organs in CathD null mice via AAV-mediated gene delivery in neonatal animals.

Keywords

near-infrared; fluorescence; lysosomal storage disease; cathepsin D; central nervous system; gene therapy; AAV; neurologic disease

Corresponding author: Bakhos A. Tannous, Ph.D., Molecular Neurogenetics Unit, Massachusetts General Hospital-East, 13th Street, Building 149, Charlestown, MA, 02129 USA, Phone 617–726–6026, Fax 617–724–1537, btannous@hms.harvard.edu.

[a]Institute for Biological and Medical Imaging, Helmholtz Zentrum Muenchen, Ingolstaedter Landstrasse 1-Neuherberg, Germany

[b]Center for Pediatric Neurology, Cleveland Clinic, Cleveland, OH

[c]Department of Radiology, Methodist Hospital Research Institute, Weill Cornell Medical College, Houston TX

[d]Department of Neurology and Gene Therapy Center, University of Massachusetts Medical School, Worcester, MA

[3]These authors contributed equally to this work.

CONFLICT OF INTEREST

The authors declare no conflict of interest.

INTRODUCTION

Lysosomal storage diseases comprise over 40 genetic deficiency states involving accumulation of undegraded gangliosides, lipids, oligosaccharides, and proteins in tissues throughout the body, with a collective incidence of 1/7500 in the population.[1,2] Many of these diseases have a predominant neurodegenerative phenotype leading to loss of mental functions and early death, such as Tay-Sachs disease.[3] The neuronal ceroid lipofuscinoses (NCLs) are a subtype of lysosomal storage diseases typically with neurodegenerative onset in childhood and accumulation of autofluorescent storage material such as lipofuscin in multiple tissues. As of 2005, six genes had been identified as underlying different forms of this condition.[4] In 2006, two groups identified disruptive mutations in the gene for the protease cathepsin D (CathD), as the underlying autosomal recessive defect in most cases of severe, congenital NCL in humans.[5,6] This lysosomal aspartyl endopeptidase is present in most tissues, with particularly high levels in the brain.[7,8] This deficiency state had previously been characterized in several naturally occurring animal models, including sheep[9] and dogs.[10,11] A knock-out mouse model of CathD deficiency develops seizures, blindness, thromboemboli, lymphopenia, and intestinal necrosis, with death occurring around postnatal day 26.[12,13,14]

Gene therapy using viral vectors to deliver the missing enzyme directly into the brain has proven very promising in experimental models of a number of lysosomal storage diseases[15,16] taking advantage of cross-correction, whereby normal cells release the deficient enzyme for uptake by endogenous deficient cells.[17] Pro-CathD is secreted from cells and can be taken up via the mannose-6-phosphate receptors for incorporation into lysosomes.[18] Adeno-associated viral (AAV) vector-mediated gene delivery to the central nervous system (CNS) has proven highly effective in a large number of small and large animal models of lysosomal storage diseases with neurological involvement.[15,16] The ability to achieve widespread, sustained gene delivery to the brain using AAV vectors, combined with their low-to-no toxicity, has supported their use in clinical trials for enzyme replacement in Canavan's disease,[19] as well as infantile and late infantile NCL[20,21] (for review see Wong *et al.*[22]).

New molecular imaging modalities provide the opportunity to image pathogenic mechanisms, gene delivery and therapeutic response in the brain and other tissues.[23] In particular, near-infrared fluorescence (NIRF) allows imaging of protease activity in cells using probes in which a fluorochrome emitting in the infrared range (with high tissue penetrance) is quenched by its positioning along a polylysine polymer through linkage to a protease peptide substrate, with cleavage of the peptide producing a marked increase in fluorescence.[24] This imaging modality has been used to monitor activity of cathepsins in tumors,[25,26] viral proteases associated with vector delivery,[27] matrix metalloproteinases in metastatic tumor foci[28] and caspases during apoptosis.[29,30]

This study focuses on gene delivery of CathD to a knock-out mouse model of congenital NCL. Intracranial and intraperitoneal (i.p.) injections of AAV2/rh8 vectors encoding mouse CathD (mCathD) were performed in newborn pups. Successful gene replacement was

observed by extended survival times and expression of CathD activity in cells and tissues as detected by CathD-specific NIRF imaging.

RESULTS

Generation and characterization of AAV vector encoding mouse cathepsin D

mCathD cDNA was cloned into an AAV vector plasmid under the control of the CBA promoter (pAAV-mCathD; Fig. 1A). As a control, a similar vector was generated expressing enhanced GFP under the same promoter (pAAV-GFP). To test for vector-mediated mCathD expression, fibroblasts from homozygous CathD knock-out embryos were transiently transfected with the pAAV-mCathD or pAAV-GFP plasmid and western blot analysis was performed on cell lysates 48 h later. In cells transfected with pAAV-mCathD, a double band was observed around 50 kDa corresponding to a short live precursor form (53 kDa) and the intermediate form (47 kDa) of CathD, as well as a band at 30 kDa corresponding to the mature form of CathD[31] (Fig. 1B). None of these bands were observed in lysates from knockout cells transfected with pAAV-GFP.

In order to image vector-mediated CathD expression, wild-type mouse fibroblasts, knockout fibroblasts, as well as knock-out fibroblasts transfected with pAAV-GFP or both pAAV-mCathD and pAAV-GFP plasmids were incubated with a Cy5.5-CathD-specific NIRF probe (200 nM for 60 min) and FACS analyzed for Cy5.5 fluorescence. The knock-out fibroblasts showed very minimal signal, while the wild-type fibroblasts showed intense Cy5.5 fluorescence, indicating that the probe was cleaved and activated in the presence of CathD in these cells (Fig. 2). Knock-out cells co-transfected with both pAAV-mCathD and pAAV-GFP plasmids showed an increase in Cy5.5 fluorescence intensity (all GFP positive cells were also Cy5.5 positive), as compared to cells transfected with pAAV-GFP plasmid alone which showed no signal (Fig. 2). These results prove that CathD gene delivery can be monitored using NIRF imaging and that the mature form of CathD is active in these cells.

Extended lifespan of knock-out mice injected with AAV2/rh8 mouse cathepsin D vector

In order to check whether mCathD gene delivery to the brain could impact survival, knock-out mice received intracerebroventricular (i.c.v.) injection at post-natal day 1 (P1; n = 16) or P4 (n = 6) with either PBS (control) or 2×10^{10} genome copies (g.c.) of AAV2/rh8-mCathD in each ventricle. We have previously shown that this dose of AAV2/rh8 vector yields widespread gene delivery in neonatal mouse brain.[32,33] Time of death was recorded. There was no significant survival benefit among the two groups (data not shown). Since loss of function of cathD in humans and mice results in death-related changes in both the brain (microcephaly, seizures) and peripheral tissues (respiratory insufficiency, massive intestinal necrosis, thromboemboli and lymphopenia), we decided to perform both cerebral ventricular, as well as i.p. injections. Neonatal pups were injected on P1 (n = 2), P2 (n = 4) or P4 (n = 4; total n = 10) with both i.c.v. (2×10^{10} g.c. in 2 μl 0.06% Trypan blue to each ventricle) and i.p. (1×10^{10} g.c. in 100 μl) of AAV2/rh8-mCathD vector. Similar group of mice were injected with PBS as a control and time of death was recorded. Control knock-out mice had an average lifespan of 29.1 (S.E. ± 0.6 days; range, 26–32 days, n = 10) consistent with previous studies.[12] AAV2/rh8-mCathD vector-injected knock-out mice had a

significantly longer average lifespan of 35.4 days (S.E. ± 2.1 days; range, 29–49 days, n = 10; Fig. 3a). No differences were seen between mice injected at different post-natal days. Knock-out mice injected with the AAV2/rh8-GFP control vector had a similar lifespan as PBS-injected mice, while injected heterozygous and wild-type littermates were healthy and lived for about two years (data not shown). In a parallel experiment, AAV2/rh8-mCathD-injected knock out mice were sacrificed at P27. Brains were removed from these mice and other knockout, heterozygous and wild-type mice, lysed and analyzed by western blotting. A double band around 50 kDa corresponding to the short lived and intermediate form of CathD as well as two bands at 31 kDa and 14 kDa corresponding to the mature fragments was observed in brain lysates from knockout mice injected with AAV2/rh8-mCathD, but not in non-injected knockout mice, showing efficient CathD gene expression in the brain (Fig. 3b). The same bands were observed in lysates from heterozygous and wild-type brains.

Imaging of cathepsin D gene replacement *ex vivo* with near-infrared fluorescence probe

Neonatal CathD pups from heterozygous matings were injected with either AAV2/rh8-mCathD vector at post-natal day 1 (as above). On post-natal day 24 (2–3 days prior to average time of mortality in knock-out animals), AAV2/rh8-mCathD or PBS treated knock-out mice (n = 6) were injected i.p. with the CathD-specific NIRF probe (0.1 nmoles/g body weight) and sacrificed 24 h later by perfusion with PBS. Liver, brain, heart, spleen and kidneys were removed and rinsed in PBS prior to imaging. Organs were imaged using a custom-built camera system[34] followed by image analysis using Kodak Digital Science 1D software (Fig. 4A). A significant increase (4-fold; $p<0.00001$; student t-test) in Cy5.5 fluorescence signal in the brains of homozygous knockout mice injected with AAV2/rh8-mCathD vector was observed as compared to PBS-injected knock-out mice (Fig. 4B). Signal in the livers of injected mice was approximately 1.5-fold higher than controls (*$p<0.0001$). No significant increase in signal was seen in the heart, kidneys, or spleen of treated mice compared to PBS control animals. In a parallel experiment, we attempted to image CathD expression in the brain non-invasively *in vivo* using planar fluorescence imaging with normalized data at different time points (2 – 24 h) after injection of the NIRF probe as described.[35,36] Unfortunately, we could not detect significant increase in Cy5.5 levels between knock-out mice injected with AAV2/rh8-mCathD vector at P1 and with the NIRF probe at P24, as compared to PBS-treated mice (n = 4) presumably due to the low sensitivity of the imaging system and the diffuse expression of the enzyme in the brain.

DISCUSSION

Relevance of findings

This is the first report of experimental gene therapy for congenital NCL, which is a severe, early onset disorder causing neuronal degeneration. An AAV2/rh8 vector encoding the replacement enzyme CathD under a strong constitutive promoter was able to express active enzyme in cultured embryonic fibroblasts from knock-out mice, as well as in brain and liver from these mice after combined infusion into the brain lateral ventricles and systemic (i.p.) in the perinatal period. Although the mice were not completely cured, gene delivery was effective in expanding the lifespan of these knock-out mice significantly using a single i.c.v. and i.p. injection of 10^{10} g.c. Systemic injection of knockout mice with a higher dose of this

AAV vector could potentially increase their survival even further. The advantage of CathD in this paradigm is that activity can be visualized and quantitated by NIRF imaging in cells and tissues using probes that have been shown to penetrate the brain efficiently[37,38]. These studies support the feasibility of AAV-mediated gene delivery for enzyme replacement in lysosomal storage disorders which affect the nervous system. Further, they illustrate a paradigm for potential monitoring of enzyme activity *in vivo* using an enhanced and more sensitive imaging system that is clinically compatible.

Gene therapy for lysosomal storage diseases

Experimental approaches to neuropathic lysosomal storage diseases include gene therapy and stem cell therapy. Of the gene therapy vectors, AAV has been translated into clinical trials for these diseases and has several advantages. These vectors can be injected directly into the brain parenchyma where they, as well as the enzymes encoded in them, can be transported over long distances via retrograde axonal transport to structures that send afferent connections to vector-transduced areas.[39,40] Neonatal i.c.v. delivery of AAV vectors, as used in this study, has proven highly efficient in mouse models of neuropathic lysosomal storage diseases, taking advantage of either interstitial fluid flow or CSF flow for distribution of lysosomal enzymes throughout the CNS.[41,42,33] This approach is appealing for translation into humans since the neurosurgical procedure involved with ICV delivery of AAV vectors should be similar to placement of shunts in the lateral ventricles, a procedure carried out routinely in children to prevent hydrocephalus.[43] Intrathecal delivery of AAV vectors has also proven very efficient for global delivery of lysosomal enzymes to the CNS.[44] AAV vectors are by far the most widely used for gene delivery to the CNS in the experimental setting in the laboratory and also for clinical translation into humans as they mediate long-term gene expression (up to 96 weeks in humans)[45] with no apparent toxicity. The increasing number of AAV serotypes and chimeric capsids provides future opportunities for more extensive delivery of genes to the brain, even across the blood-brain barrier (BBB).[46] Presently, we do not know the exact cause of death of AAV-treated knock-out mice, but given that this enzyme is expressed throughout the body and that symptoms of CathD deficiency are widespread, we speculate that this may be due to insufficient replacement of CathD in multiple tissues throughout the body.

Imaging gene delivery

Molecular imaging allows a visual (often quantitative) representation of molecular, cellular, biochemical and physiological processes in a living organism. Optical imaging, in particular fluorescence imaging, provides a facile and rapid way to image specific molecular events *in vivo*. Fluorescent probes emitting in the near-infrared (NIR) spectrum offer the advantages of deeper tissue penetration, since there is minimal hemoglobin absorption, and improved signal-to-background ratio as autofluorescence from nontarget tissues is low. Recently, NIRF fluorochrome coupled to quenching peptides which are cleaved in response to activation of different enzymes have been used successfully for the detection of several proteases, such as cathepsins and caspases.[47,48,29,49] These probes have been used both in pre-clinical and clinical trials Although in this study, we could not reproducibly image expression of CathD in the brain *in vivo*, we were able to detect the signal in tissues *ex vivo* after *in vivo* delivery. Advancement in the field of fluorescence imaging by developing more

sophisticated instrumentation and reconstruction methods should allow detection of CathD activity in the future. Recently, state-of-the-art hybrid imaging systems for Fluorescence and X-Ray Tomography (FMT-XCT) can reconstruct and co-register in 3D both the anatomical and the functional information. This improvement in fluorescence 3D imaging has been demonstrated using a NIR probe to target the amyloid-beta plaques in the brains of mice models in Alzheimer's disease.[50]

Implications for future

Gene therapy for metabolic deficiency states appears especially promising for diseases in which cross-correction is possible, as gene delivery *in vivo* is intrinsically limited to a subpopulation of cells. Further, in the case of lysosomal storage diseases, it appears that restoration of even 10% of enzyme activity can have marked therapeutic efficacy in animal models. Direct gene delivery to the brain is important in diseases affecting the nervous system as entry into the brain from the periphery is limited by the BBB. In particular, AAV vectors are useful in this context as they have low-no toxicity, are stable and have a small size allowing spread within tissues, with some serotypes preferentially infecting neurons. Early intervention is considered critical to protecting the brain from neurodegenerative changes. Use of replacement enzymes for which activity can be measured in living cells and *in vivo* using new molecular imaging methods will provide the opportunity to optimize delivery systems. The present study provides a basis for further consideration of gene therapy for congenital NCL.

METHODS

Generation of AAV vector

An AAV vector, pAAV-mCathD was derived from the plasmid pAAV-CBA-MBG-W[32] by removing the MBG cassette and replacing it with the mCathD cDNA (1893 bp) excised from a pBluescript clone (ATTC construct CD-3a, number 63114). mCathD was placed under the control of the strong, constitutive hybrid cytomegalovirus (CMV) enhancer/chicken beta-actin promoter (CBA).[51] A similar vector expression GFP (pAAV-GFP) was used as a control.[32] AAV2/rh8 vectors were produced by co-transfection of 293T cells by calcium phosphate precipitation of vector plasmid (pAAV-mCathD), a mini-adenovirus helper plasmid pFΔ6 (from Dr. Weidong Xiao, Univ. Penn. Med. Ctr., Philadelphia, PA), and AAVrh8 helper plasmid pAR8.[32] AAV2/rh8 vectors were purified and titered, as described[32] yielding typical titers of 2.8×10^{14} g.c. per ml.

Source and breeding of cathepsin D knock-out mice

The CathD knock-out line was obtained from Dr. Paul Saftig (University Kiel, Germany) via Dr. Hidde Ploegh (Harvard Medical School). Mice heterozygous for the disrupted CathD gene contain a neomycin cassette insertion in exon 4.[12] Mice homozygous for the mutation were generated by breeding heterozygous mice yielding a frequency of approximately 25% affected pups per litter. Mice were genotyped at 3 weeks of age by PCR of tail clip DNA using two sets of primers in parallel. MCD14 (5′-AGACTAACAGGCCTGTTCCC-3′) and MCD15 (5′-TCAGCTGTAGTTGCTCACATG-3′), and AK30 (5′-CGGATCAAGCGTATGCAGCCG-3′) and AK31 (5′-

CAAGATGGATTGCACGCAGG-3′).[52] MCD14 and MCD15 amplify a 200 bp fragment inside the wild-type allele and a 1400 bp fragment in the mutant allele. AK30 and AK31 amplify a 400 bp fragment within the wild-type allele.

Generation and cell culture of mouse embryonic fibroblasts

Mouse embryonic fibroblasts (MEFs), homozygous and heterozygous for the mutant CathD gene, were generated from E17 embryos, as described.[53] These cells spontaneously immortalized and were grown in Dulbecco's modified Eagle's medium (DMEM) supplemented with 10% fetal bovine serum (Sigma, St. Louis, MO), 100 U penicillin and 0.1 mg per ml streptomycin (Sigma), at 37°C in a5% CO2 in a humidified atmosphere.

SDS-gel electrophoresis and western blotting

Cells were transiently transfected with DNA expression constructs using the calcium phosphate transfection method. Forty-eight h post-transfection, total cell lysates were prepared by washing the cells twice with PBS and resuspending the cell pellet in lysis buffer containing 50 mM Tris-HCL, pH 7.4, 0.25% sodium deoxycholate, 150 mM NaCl, 1 mM EGTA, 1 mM phenylmethylsulphonyl fluoride 1 μg/mL pepstatin, 1 mM Na3Vo4, 1 mM NaF, 10% NP-40 and protease inhibitors (PI Complete; Roche Diagnostics). Lysates from mice brain were prepared by homogenizing brains using a pellet pestle motor (Kontes) in 300 μl of M-PER mammalian protein extraction reagent (Thermo Scientific). Fifty μg protein were resolved by electrophoresis in a 4 – 20 % gradient SDS-polyacrylamide gel. Proteins were transferred electrophoretically to nitrocellulose (Bio-Rad, Hercules, CA) and stained for protein with 0–2% Ponceau S (Sigma). The membrane was blocked over night in 5% non-fat milk powder in TBST (150 mm NaCl, 50 mM TRIS, pH 8, 0.1% TWEEN). The blot was probed with an antibody against CathD (Santa Cruz Biotechnologies, Inc., Santa Cruz, CA; SC-6486) diluted 1:100 in 5% milk in TBST, or beta-actin followed by secondary antibody conjugated to horse radish peroxidase diluted 1:2500 in 5% milk in TBST (Sigma) and visualized with Super Signal West Pico Chemiluminescent Substrate TM (Pierce Biotechnology, Rockford, IL).

FACS analysis

CathD knock-out MEFs were transfected with either pAAV-GFP (3 μg) or both pAAV-mCathD (3 μg) and pAAV-GFP (1 μg) plasmids using Lipofectamine (Invitrogen). Forty-eight h later, these cells and wild-type MEFs were treated for 1 h at 37°C with 200 nM of a cyanine Cy5.5-CathD NIRF probe.[26] Cells were washed once with PBS, then aspirated and resuspended in PBS and analyzed for both GFP and NIRF fluorescence using a FACS-Calibur cytometer (Becton Dickinson, San Jose, CA).

Vector injections into mice and survival curves

Heterozygous CathD knock-out mice were mated and neonatal pups were cryoanesthetized on postnatal day 1–4 (P1-4). Pups were injected with 2 μl viral vector (2×10^{10} g.c. in 0.06% Trypan blue) into each of the cerebral ventricles using a glass micropipetter (70–100 μm in diameter) and a Narishige IM300 microinjector. Trypan blue allowed us to visualize the ventricles being filled with the virus. The same mice were also i.p. injected with 100 μl

(1×10^{10} g.c.) of the same viral vector using a 1 mL syringe and 30 gauge needle as a control, mice received similar injections of PBS only. Mice were then placed on a warming pad and returned to the mothers after regaining normal color and full activity typical of newborn mice. Mice were genotyped at approximately three weeks of age and knock-outs observed for onset and progression of symptoms and date of death. Uninjected mice were also observed in parallel. The experimental protocol was approved by the Institutional Animal Care and Use Committee at Massachusetts General Hospital and followed guidelines set forth in the National Institute of Health Guide for the Care and Use of Laboratory Animals. Survival data was analyzed using a Kaplan-Meier plot. Statistical evaluation was performed using JMP statistical software with the significance calculated by log-rank.

Cathepsin D NIRF imaging

Pups from mating of heterozygous CathD knock-out mice were injected i.c.v. and i.p. with AAV2/rh8-mCathD or PBS on P1, as above (n = 6). On P24, AAV-mCathD treated and control mice were injected i.p. with the NIRF probe (0.1 nmoles/g body weight) and sacrificed 24 h later by perfusion with PBS. Liver, brain heart, spleen and kidneys were removed and rinsed in PBS prior to imaging. Organs were imaged using a custom-built camera system[34] at 5 defined regions of interest in each organ followed by image analysis using Kodak Digital Science 1D software (Kodak).

Acknowledgments

This work was supported by a Howard Hughes Fellowship (GH), NIH/NINDS NS24279 (XOB) and NS045776 (BAT), as well as NIH/NCI CA86355 (XOB and BAT). We thank Ms. Suzanne McDavitt for skilled editorial assistance.

References

1. Hodges BL, Cheng SH. Cell and gene-based therapies for the lysosomal storage diseases. Curr Gene Ther. 2006; 6:227–241. [PubMed: 16611044]
2. Vellodi A. Lysosomal storage disorders. Br J Haematol. 2005; 128:413–431. [PubMed: 15686451]
3. Fernandes Filho JA, Shapiro BE. Tay-Sachs disease. Arch Neurol. 2004; 61:1466–1468. [PubMed: 15364698]
4. Mole SE, Williams RE, Goebel HH. Correlations between genotype, ultrastructural morphology and clinical phenotype in the neuronal ceroid lipofuscinoses. Neurogenetics. 2005; 6:107–126. [PubMed: 15965709]
5. Siintola E, Partanen S, Stromme P, Haapanen A, Haltia M, Maehlen J, et al. Cathepsin D deficiency underlies congenital human neuronal ceroid-lipofuscinosis. Brain. 2006; 129:1438–1445. [PubMed: 16670177]
6. Steinfeld R, Reinhardt K, Schreiber K, Hillebrand M, Kraetzner R, Bruck W, et al. Cathepsin D deficiency is associated with a human neurodegenerative disorder. Am J Hum Genet. 2006; 78:988–998. [PubMed: 16685649]
7. Whitaker JN, Rhodes RH. The distribution of cathepsin D in rat tissues determined by immunocytochemistry. Am J Anat. 1983; 166:417–428. [PubMed: 6344609]
8. Reid WA, Valler MJ, Kay J. Immunolocalization of cathepsin D in normal and neoplastic human tissues. J Clin Pathol. 1986; 39:1323–1330. [PubMed: 3543065]
9. Palmer DN, Husbands DR, Winter PJ, Blunt JW, Jolly RD. Ceroid lipofuscinosis in sheep. I. Bis(monoacylglycero)phosphate, dolichol, ubiquinone, phospholipids, fatty acids, and fluorescence in liver lipopigment lipids. J Biol Chem. 1986; 26:1766–1772. [PubMed: 3944107]

10. Awano T, Katz ML, O'Brien DP, Taylor JF, Evans J, Khan S, et al. A mutation in the cathepsin D gene (CTSD) in American Bulldogs with neuronal ceroid lipofuscinosis. Mol Genet Metab. 2006; 87:341–348. [PubMed: 16386934]
11. Drogemuller C, Wohlke A, Distl O. Characterization of candidate genes for neuronal ceroid lipofuscinosis in dog. J Hered. 2005; 96:735–738. [PubMed: 15958790]
12. Saftig P, Hetman M, Schmahl W, Weber K, Heine L, Mossmann H, et al. Mice deficient for the lysosomal proteinase cathepsin D exhibit progressive atrophy of the intestinal mucosa and profound destruction of lymphoid cells. EMBO J. 1995; 14:3599–3608. [PubMed: 7641679]
13. Koike M, Nakanishi H, Saftig P, Ezaki J, Isahara K, Ohsawa Y, et al. Cathepsin D deficiency induces lysosomal storage with ceroid lipofuscin in mouse CNS neurons. J Neurosci. 2000; 20:6898–6906. [PubMed: 10995834]
14. Koike M, Shibata M, Waguri S, Yoshimura K, Tanida I, Kominami E, et al. Participation of autophagy in storage of lysosomes in neurons from mouse models of neuronal ceroid-lipofuscinoses (Batten disease). Am J Pathol. 2005; 167:1713–1728. [PubMed: 16314482]
15. Sands MS, Davidson BL. Gene therapy for lysosomal storage diseases. Mol Ther. 2006; 13:839–849. [PubMed: 16545619]
16. Schiffmann R. Therapeutic approaches for neuronopathic lysosomal storage disorders. J Inherit Metab Dis. 2010; 33:373–379. [PubMed: 20162366]
17. Kroll RA, Neuwald EA. Outwitting the blood-brain barrier for therapeutic purposes: osmotic opening and other means. Neurosurgery. 1998; 42:1082–1099.
18. Pohlmann R, Boeker MW, von Figura K. The two mannose 6-phosphate receptors transport distinct complements of lysosomal proteins. J Biol Chem. 1995; 270:27311–27318. [PubMed: 7592993]
19. McPhee SW, Janson CG, Li C, Samulski RJ, Camp AS, Francis J, et al. Immune responses to AAV in a phase I study for Canavan disease. J Gene Med. 2006; 8:577–588. [PubMed: 16532510]
20. Crystal RG, Sondhi D, Hackett NR, Kaminsky SM, Worgall S, Stieg P, et al. Clinical protocol. Administration of a replication-deficient adeno-associated virus gene transfer vector expressing the human CLN2 cDNA to the brain of children with late infantile neuronal ceroid lipofuscinosis. Hum Gene Ther. 2004; 15:1131–1154. [PubMed: 15610613]
21. Griffey M, Bible E, Vogler C, Levy B, Gupta P, Cooper J, et al. Adeno-associated virus 2-mediated gene therapy decreases autofluorescent storage material and increases brain mass in a murine model of infantile. Neurobiol Dis. 2004; 16:360–369. [PubMed: 15193292]
22. Wong AM, Rahim AA, Waddington SN, Cooper JD. Current therapies for the soluble lysosomal forms of neuronal ceroid lipofuscinosis. Biochem Soc Trans. 2010; 38:1484–1488. [PubMed: 21118112]
23. Shah K, Jacobs A, Breakefield XO, Weissleder R. Molecular imaging of gene therapy for cancer. Gene Ther. 2004a; 11:1175–1187. [PubMed: 15141158]
24. Funovics M, Weissleder R, Tung CH. Protease sensors for bioimaging. Anal Bioanal Chem. 2003; 377:956–963. [PubMed: 12955390]
25. Weissleder R, Tung CH, Mahmood U, Bogdanov AJ. In vivo imaging of tumors with protease-activated near-infrared fluorescent probes. Nat Biotechnol. 1999; 17:375–378. [PubMed: 10207887]
26. Tung CH, Mahmood U, Bredow S, Weissleder R. In vivo imaging of proteolytic enzyme activity using a novel molecular reporter. Cancer Res. 2000; 60:4953–4958. [PubMed: 10987312]
27. Shah K, Tung CH, Chang CH, Slootweg E, O'Loughlin T, Breakefield XO, et al. *In vivo* imaging of HIV protease activity in amplicon vector-transduced gliomas. Cancer Res. 2004b; 64:273–278. [PubMed: 14729634]
28. Bremer C, Tung CH, Weissleder R. Molecular imaging of MMP expression and therapeutic MMP inhibition. Acad Radiol. 2002; 2:S314–315. [PubMed: 12188259]
29. Messerli SM, Prabhakar S, Tang Y, Shah K, Cortes ML, Murthy V, et al. A novel method for imaging apoptosis using a caspase-1 near-infrared fluorescent probe. Neoplasia. 2004; 6:95–105. [PubMed: 15140398]
30. Pham W, Weissleder R, Tung CH. An azulene dimer as a near-infrared quencher. Angew Chem Int Ed Engl. 2002; 41:3659–3662. [PubMed: 12370922]

31. Rijinboutt S, Stoorvogel W, Geuze HJ, Strous GJ. Identification of subcellular compartments involved in biosynthetic processing of cathepsin d. J Biol Chem. 1992; 267:15665–15672. [PubMed: 1322403]
32. Broekman ML, Comer LA, Hyman BT, Sena-Esteves M. Adeno-associated virus vectors serotyped with AAV8 capsids are more efficient than AAV-1 or -2 serotypes for widespread gene delivery to the neonatal mouse brain. Neuroscience. 2006; 138:501–510. [PubMed: 16414198]
33. Broekman ML, Baek RC, Comer LA, Fernandez JL, Seyfried TN, Sena-Esteves M. Complete Correction of Enzymatic Deficiency and Neurochemistry in the GM1-gangliosidosis Mouse Brain by Neonatal Adeno-associated Virus-mediated Gene Delivery. Mol Ther. 2007; 15:30–37. [PubMed: 17164772]
34. Mahmood U, Tung CH, Bogdanov AJ, Weissleder R. Near-infrared optical imaging of protease activity for tumor detection. Radiology. 1999; 213:866–870. [PubMed: 10580968]
35. Ntziachristos V, Turner G, Dunham J, Windsor S, Soubret A, Ripoll J, et al. Planar fluorescence imaging using normalized data. J Biomed Opt. 2005; 10:064007. [PubMed: 16409072]
36. Haller J, Hyde D, Deliolanis N, de Kleine R, Niedre M, Ntziachristos VJ. Visualization of pulmonary inflammation using noninvasive fluorescence molecular imaging. Appl Physiol. 2008; 104:795–802.
37. Okamura N, Mori M, Furumoto S, Yoshikawa T, Harada R, Ito S, et al. In vivo detection of amyloid plaques in the mouse brain using the near-infrared fluorescence probe THK-265. J Alzherimers Dis. 2011; 23:37–48.
38. Klohs J, Baeva N, Steinbrink J, Bourayou R, Boettcher C, Royl G, et al. In vivo near-infrared fluorescence imaging of matrix metalloproteinase activity after cerebral ischemia. J Cereb Blood Flow Metab. 2009; 29:1284–1292. [PubMed: 19417756]
39. Passini MA, Lee EB, Heuer GG, Wolfe JH. Distribution of a lysosomal enzyme in the adult brain by axonal transport and by cells of the rostral migratory stream. J Neurosci. 2002; 22:6437–6446. [PubMed: 12151523]
40. Cearley CN, Wolfe JH. A single injection of an adeno-associated virus vector into nuclei with divergent connections results in widespread vector distribution in the brain and global correction of a neurogenetic disease. J Neurosci. 2007; 27:9928–9940. [PubMed: 17855607]
41. Passini MA, Watson DJ, Vite CH, Landsburg DJ, Peigenbaum AL, Wolfe JH. Intraventricular brain injection of adeno-associated virus type 1 (AAV1) in neonatal mice results in complementary patterns of neuronal transduction to AAV2 and total long-term correction of storage lesions in the brains of beta-glucuronidase-deficient mice. J Virol. 2003; 77:7034–7040. [PubMed: 12768022]
42. Passini MA, Wolfe JH. Widespread gene delivery and structure-specific patterns of expression in the brain after intraventricular injections of neonatal mice with an adeno-associated virus vector. J Virol. 2001; 25:12382–12392. [PubMed: 11711628]
43. Rudolph D, Sterker I, Graefe G, Till H, Ulrich A, Geyer C. Visual field constriction in children with shunt-treated hydrocephalus. J Neurosurg Pediatr. 2010; 6:481–485. [PubMed: 21039173]
44. Watson G, Bastacky J, Belichenko P, Buddhikot M, Jungles S, Vellard M, et al. Intrathecal administration of AAV vectors for the treatment of lysosomal storage in the brains of MPS I mice. Gene Ther. 2006; 13:917–925. [PubMed: 16482204]
45. Muramatsu S, Fujimoto K, Kato S, Mizukami H, Asari S, Ikeguchi K, et al. A phase I study of aromatic L-amino acid decarboxylase gene therapy for Parkinson's disease. Mol Ther. 2010; 18:1731–1735. [PubMed: 20606642]
46. Gray SJ, Woodard KT, Samulski RJ. Viral vectors and delivery strategies for CNS gene therapy. Therapeutic Delivery. in press.
47. Jaffer FA, Vinegoni C, John MC, Aikawa E, Gold HK, Finn AV, et al. Real-time catheter molecular sensing of inflammation in proteolytically active atherosclerosis. Circulation. 2008; 118:1802–1809. [PubMed: 18852366]
48. Blum G, von Degenfeld G, Merchant MJ, Blau HM, Bogyo M. Noninvasive optical imaging of cysteine protease activity using fluorescently quenched activity-based probes. Nat Chem Biol. 2007; 3:668–677. [PubMed: 17828252]

49. Maxwell D, Chang Q, Zhang X, Barnett EM, Piwnica-Worms D. An improved cell-penetrating, caspase-activatable, near-infrared fluorescent peptide for apoptosis imaging. Bioconjug Chem. 2009; 20:702–709. [PubMed: 19331388]

50. Hyde D, de Kleine R, MacLaurin SA, Miller E, Brooks DH, Krucker T, et al. Hybrid FMT-CT imaging of amyloid-beta plaques in a murine Alzheimer's disease model. Neuroimage. 2009; 44:1304–1311. [PubMed: 19041402]

51. Xu L, Daly T, Gao C, Flotte TR, Song S, Byrne BJ, et al. CMV-beta-actin promoter directs higher expression from an adeno-associated viral vector in the liver than the cytomegalovirus or elongation factor 1 alpha promoter and results in therapeutic levels of human factor X in mice. Hum Gene Ther. 2001; 12:563–572. [PubMed: 11268288]

52. Saftig P, Peters C, von Figura K, Craessaerts K, Van Leuvan F, De Strooper B. Amyloidogenic processing of human amyloid precursor protein in hippocampal neurons devoid of cathepsin D. J Biol Chem. 1996; 271:27241–27244. [PubMed: 8910296]

53. Bakowska JC, Di Maria MV, Camp SM, Wang Y, Allen PD, Breakefield XO. Targeted transgene integration into transgenic mouse fibroblasts carrying the full-length human AAVS1 locus mediated by HSV/AAV rep(+) hybrid amplicon vector. Gene Ther. 2003; 10:1691–1702. [PubMed: 12923568]

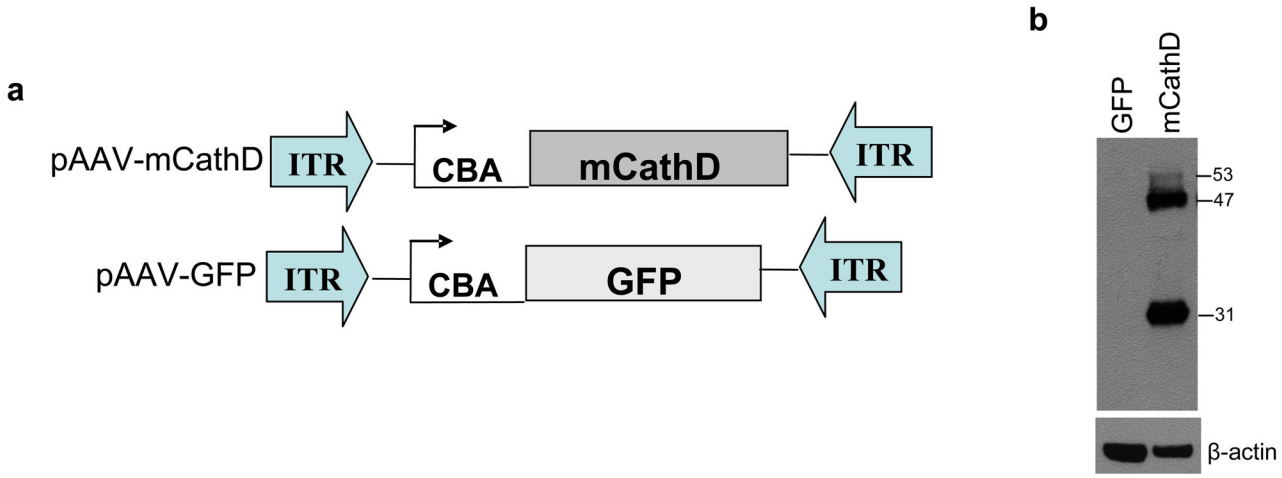

Figure 1. AAV constructs and gene delivery of CathD to knock-out MEFs

(a) Maps of pAAV constructs expressing mouse CathD (mCathD) cDNA or GFP under control of the strong constitutively active CBA promoter. (**b**) MEF −/− knock-out cells were transfected with pAAV-mCathD or pAAV-GFP. Forty-eight h later, cells were lysed and analyzed by SDS-PAGE and western blotting using anti-CathD antibody and β-actin for loading efficiency. Showing is a representative blot from 3 independent experiments all yielding similar results.

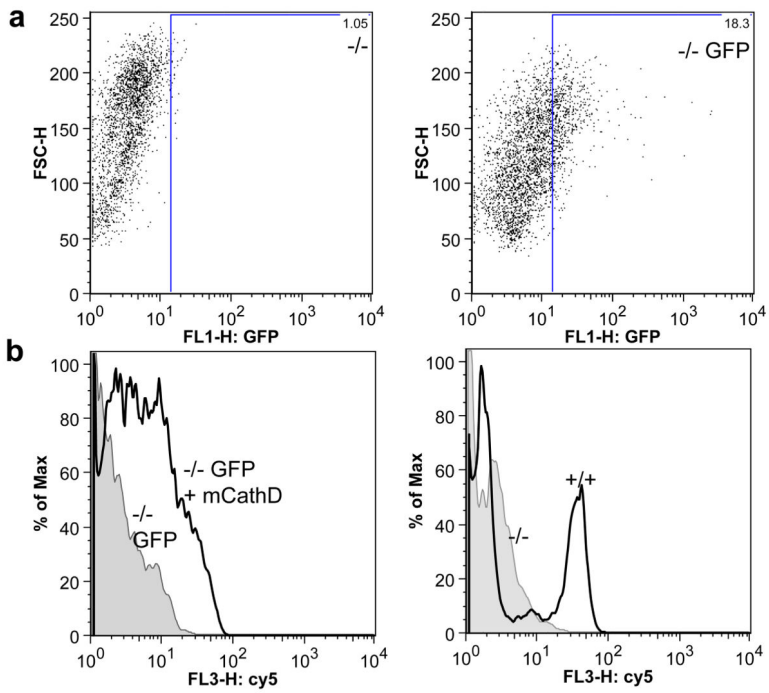

c

	GFP	CY5	
	% cells	**% cells**	**MFI**
-/- GFP	15.2 ± 3.2	N/A	N/A
-/- GFP + mCathD	16.1 ± 4.1	14.8 ± 4.8	1045 ± 224
+/+	N/A	44.4 ± 3.2	1232 ± 153

Figure 2. NIRF imaging of CathD in cultured cells

(**a**) Knock-out (−/−) MEFs were transfected with pAAV-GFP and 48 hours later analyzed for GFP expression. Typical dot-plot showing the transfection efficiency of MEFs being around 18%. (**b–c**) knockout cells transfected with pAAV-GFP or both pAAV-mCathD and pAAV-GFP. Forty-eight h later, these cells as well as plain knockout and wild-type (+/+) MEFs were incubated with the CathD-specific NIRF probe and analyzed by FACS 1 h later. (**b**) Representative histograms showing an intense Cy5.5 fluorescence in knockout MEFs transfected with pAAV-mCathD and pAAV-GFP as well as in wild-type MEFs, but not in knock-out MEFs transfected with pAAV-GFP. (**c**) Quantitation analysis of FACS data from three independent experiments. MFI = mean fluorescence intensity.

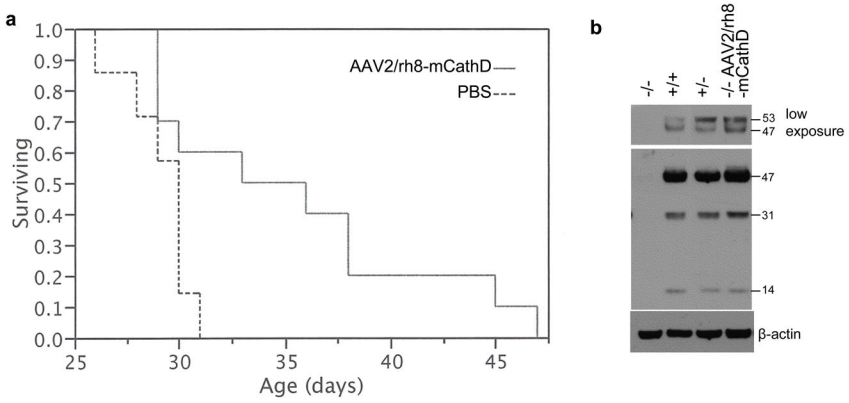

Figure 3.

AAV2/rh8-mCathD vector provides efficient gene delivery and increased survival of knock-out mice.(**A**) Neonatal pups were injected with PBS or AAV2/rh8-mCathD vector both i.c.v. (2×10^{10} g.c to each ventricle in 2 μl 0.06% Trypan blue) and i.p. (1×10^{10} g.c in 100 μl) once between P1-4 (n = 10). Time of death was recorded. The data is presented as a Kaplan-Meier survival curve of CathD knock-out mice from both groups using JMP Software. Log-rank, as well as Wilcoxon test was performed to compare mean survival of AAV2/rh8-mCathD-treated mice versus PBS control knock-out mice and the extension of survival by treatment with AAV2/rh8-mCathD was significant (Log-Rank $p \leq 0.02$; Wilcoxon $p \leq 0.05$.). The same experiment was repeated three times and similar results were obtained. (**B**) Neonatal pups were injected with AAV2/rh8-mCathD at P1 as in (A) and sacrificed at P27. Brain from these mice as well as from non-injected knockout, heterozyous and wild-type mice were removed, lysed and 50 μg protein was analyzed by western blotting for mCathD expression. The short live 53 kDa precursor of CathD is processed into the 47 kDa intermediate form and the mature enzyme composed of 31 kDa and 14 kDa fragment.

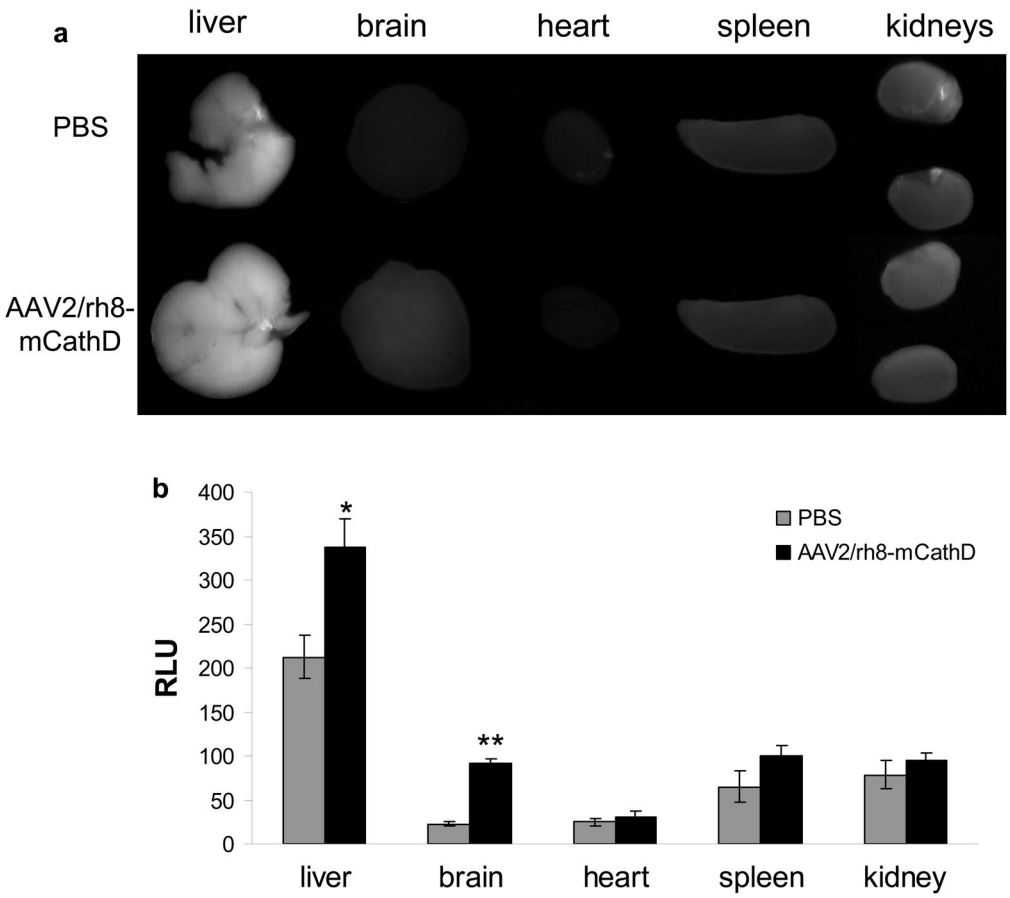

Figure 4.

NIRF imaging of CathD activity *ex vivo*. Neonatal pups were injected with AAV2/rh8-mCathD vector both i.c.v. (2×10^{10} g.c into each ventricle in 2 μl 0.06% Trypan blue) and i.p. (1×10^{10} g.c in 100 μl) on P1. Similar groups of mice were injected with PBS (n = 6/group). On P24 (2–3 days prior to mortality in knock-out animals), mice were injected i.p. with NIRF probe (0.1 nmoles/g body weight) and sacrificed 24 h later with PBS perfusion. Liver, brain, heart, spleen and kidneys were removed, rinsed with PBS, and imaged at 5 different regions of interests using a custom-built camera system followed by image analysis using Kodak Digital Science 1D software. B).(**A**) representative organs from a single mouse in each group is shown.(**B**) Signal intensity is expressed as the average relative light units (RLU) ± S.D. (n = 6). Significant increases in AAV-mCathD treated animals were seen for liver (*p<0.0001) and brain (**p<0.00001) as calculated by student t-test.